Microfabricated electrochemical gas sensor

Pierre-Alexandre Gross[1,2] ✉, *Tom Larsen*[1], *Frédéric Loizeau*[1], *Thomas Jaramillo*[3], *Denis Spitzer*[2], *Beth Pruitt*[1]

[1]*Stanford Department of Mechanical Engineering, Microsystems Laboratory, Stanford, CA, USA*
[2]*NS3E, UMR 3208 ISL/CNRS/UNISTRA, Saint-Louis, France*
[3]*Stanford Department of Chemical Engineering, Jaramillo Group, Stanford, CA, USA*
✉ *E-mail: pialgr@stanford.edu*

Published in Micro & Nano Letters; Received on 15th June 2016; Revised on 12th August 2016; Accepted on 17th August 2016

The fabrication and working principle of an electrochemical gas sensor for direct gas phase detection of organic molecules is presented. The sensor is composed of two Pt electrodes where redox reactions can occur, and an ion exchange membrane to conduct H^+ from an electrode to the other. As proton exchange membrane they used a spin-coated *Nafion*® layer. An underlying SU-8 layer assures a double role of adhesion of the *Nafion* to the substrate and water reservoir to limit dehydration of the *Nafion*. The sensor is characterised for its electrochemical properties and tested for the detection of CO as model pollutant. The detection tests are performed in the form of cyclic voltammetry, and show that the sensor can detect the gas at the applied voltage corresponding to the oxidation potential of CO into CO_2.

1. Introduction: Detection of toxic and hazardous airborne pollutants needs the development of small and cheap chemical gas sensors. Sources of the target molecules include, but are not limited to, paints, glues, exhaust pipes, solvents etc. Moreover, such technology is also suitable for the detection of trace amount of explosives.

One of the most promising and developed approach for this technology is based on the measurement of a resistance change between two electrodes as a chemical specie adsorbs on the medium in between them [1–4]. The sensing layer is usually a semiconducting metal–oxide such as ZnO [1], CuO [2], TiO_2 [3] and SnO_2 [4]. The sensing layer is heated to a high temperature (about 300°C) by a heater situated underneath which induces an increase in the concentration of reactive oxygen ions at the surface of the semiconductor [5]. These anions react with the adsorbed pollutant inducing a variation in electron conductivity in the material, and thus a resistance variation.

Besides being completely compatible with conventional microfabrication processes, this type of sensor also benefits from all the various nanofabrication techniques developed for metal oxides to increase substantially their sensitivity [6]. However, to achieve any degree of selectivity, it is necessary to combine several of these sensors, in an array, with different sensing layers [7].

A possible approach to achieve selective detection is to use the redox potential, which is characteristic to any chemical specie. To do that, the species are oxidised or reduced in an electrochemical cell configuration. When the applied voltage corresponds to the redox potential of the specie adsorbed on the electrodes, the electron exchange induces a change in current which can be measured. This signal allows for identification of the specie, as well as its quantification.

The main components of an electrochemical cell are as follows:

- One working and one counter electrode where the redox reactions will occur.
- A reference electrode, to allow identification of the species involved in the redox reactions.
- An electrolyte containing the species to be reduced or oxidised.
- A membrane which role is to separate the two electrodes and conduct ions, resulting from the redox reactions, from one to the other.

The simplest design requires only two electrodes to achieve oxidation or reduction of chemical species. However, it is necessary to have a third electrode, the reference electrode, to be able to identify the specie being oxidised or reduced. This electrode is composed of a redox couple whose redox potential is well known and does not vary in the experimental conditions. By measuring the voltage between that reference electrode and the working electrode, one can identify the species engaged in the electrochemical reaction on the working electrode, thanks to the Nernst equation.

To detect molecules in the gas phase using this principle without using any liquid electrolyte, a fully solid-state electrochemical cell must be developed. The main challenge is the incorporation of the membrane in the fabrication process.

Possible materials for the membrane include ionic conducting hydrogels [8], zirconia-based materials [9] or ionic conductive polymers such as *Nafion*®. *Nafion* is a proton conducting membrane used in proton exchange membrane fuel cells which operate by reducing O_2 and oxidising H_2 in acidic conditions [10]. One major advantage of *Nafion* is that it conducts H^+ at room temperature. It is a polymer whose monomer is composed of a *teflon*-like backbone chain and a sulphonic head. When hydrated, it forms clusters around water [11], and when acidified the sulphonic groups allow proton transportation [12].

Besides of being used in conventional fuel cells as described earlier, *Nafion* is also a promising material to be used in microfuel cells where it is used to separate the cathode and the anode while transporting protons [13]. The design developed in these devices [14] has largely inspired the present Letter.

We present a sensor that demonstrates the feasibility of the electrochemical analysis of organic species dissolved in the gas phase. As target molecule to detect, we used CO. To obtain a fully solid-state sensor, we used *Nafion* as an ionic conductive electrolyte and Pt electrodes. We choose Pt because of its well-studied electrochemical and electrocatalytic properties. The poisoning of Pt by CO, in fuel cells, is also well documented [15, 16].

We suggest that the detection of CO is based on the electrochemical reactions (i) at the working electrode and (ii) at the counter electrode. These reactions occur only when the voltage applied to the electrodes corresponds to the redox potential of the species engaged in the reactions, which is why the voltage has to be

doi: 10.1049/mnl.2016.0364

swept between the electrodes

$$CO + H_2O \rightarrow CO_2 + 2H^+ + 2e^- \quad (1)$$

$$2H^+ + 2e^- \rightarrow H_2 \quad (2)$$

We propose the following sensing mechanism:

(i) Adsorption of CO on Pt.

(ii) Oxidation of CO into CO_2 when the right voltage is applied.

(iii) Desorption of CO_2, migration of the H^+ through the *Nafion* and migration of electrons through the electrical circuit leading to an observable current signal.

(iv) Reduction of H^+ into H_2 at the other electrode.

(v) Desorption of H_2.

Since there are only two electrodes on the sensor, oxidation of CO into CO_2 occurs alternatively on both electrodes as the polarity changes during the voltage cycling. The signal of H^+ being reduced into H_2 is not expected to be observed.

2. Experimental section

2.1. Design of the sensor: The sensor has been designed with a few considerations in mind. First, the fabrication steps should impact the least possible the *Nafion* layer to keep its chemical integrity. In terms of redox reactions, the key features are the 'triple points', which are the interfaces where Pt, *Nafion* and the gas phase meet. With this in mind, the Pt electrodes do not need to be very thick, and it is anticipated that their thickness will not impact the sensitivity significantly. However, the main constraint for the geometry is the separation between the electrodes fingers because the ionic conductivity of *Nafion* starts to drop above 500 µm. Keeping the design simple is also necessary to prove that the proposed sensing mechanism might be compatible with mass production.

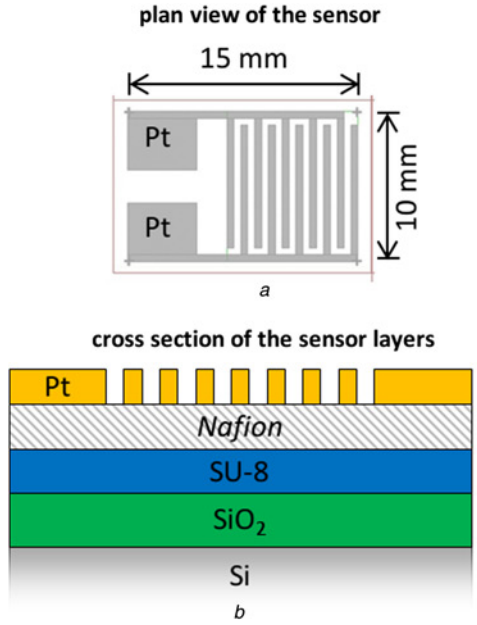

Fig. 1 *Fabrication process*
a Sensor is composed of two interdigitated Pt electrodes, each comb is 40 µm wide
b Nafion layer allows transportation of H^+ and the SU-8 serves as adhesion layer and water reservoir to prevent the dehydration of the *Nafion*

Table 1 Measured thicknesses of the different layers composing the sensor. For all layers, the measured thickness is acceptable compared with the target. For *Nafion* however, the high irregularity of the thickness across the wafer affected the yield of sensors per wafers

Layer	Target (nm)	Measured (nm)
Oxide – SiO_2	1000	920
Adhesion – SU-8	10000	9600
Membrane – *Nafion*	300	300–600
Electrodes – Pt	100	100–110

2.2. Fabrication process: First, 100 mm diameter, 525 µm thick Si wafers were processed with standard cleaning procedure in the following order: (i) 90% H_2SO_4/H_2O_2 (piranha), (ii) 5:1:1 H_2O:H_2O_2:NH_4OH, (iii) 50:1 HF (iv) 5:1:1 H_2O:H_2O_2:HCl (diffusion clean). A 1 µm thick Si oxide layer is then grown on the substrate by wet oxidising at 1100°C for 2 h 15 min.

Our studies have showed that *Nafion* adheres poorly to the SiO_2 substrate. However, it adheres well to SU-8, which can also serve as a source of water for the *Nafion,* since it is known to swell when immersed in water [17]. Thus, 10 µm thick SU-8 *2010* layer was first spin coated on the substrate at 1500 rpm for 5 s and 3000 rpm for 15 s. The layer is then exposed to a 119 mJ cm^{-2} dose of 365 nm ultraviolet (UV) light, baked at 85°C for 2 min to ensure hardening and drying of the SU-8 and then developed. Prior to deposition of the *Nafion* layer, the SU-8 coated substrate is subjected to 30 s of O_2 plasma etching.

The *Nafion* layer is deposited by spin coating a *Nafion*® *D1021* aqueous dispersion in three consecutive identical steps, which have been optimised to obtain a thickness of 300 nm, of 5 s at 500 rpm followed by 30 s at 1500 rpm. Each spin-coating step is followed by a 2 min bake at 65 °C. The deposition process is finished by a 1 h baking at 110 °C to ensure evaporation of all solvents. The electrodes are defined on the polymer coated wafer via a standard lift-off process. The HMDS treatment usually performed prior to the coating of the resist is skipped to avoid any chemical modification of the *Nafion* layer. A 3 µm thick SPR220-3 photoresist is spin coated and baked at 90 °C for 2 min. The wafer is then exposed to a 450 mJ cm^{-2} dose of 365 nm UV light, through a transparency mask displaying the geometry of the

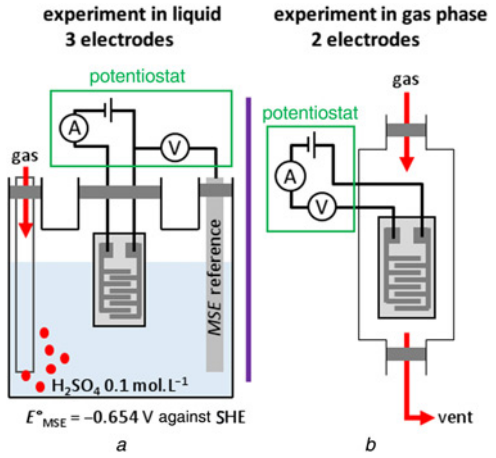

Fig. 2 *Characterisation and test methods*
a Three-electrodes configuration used for electrochemical characterisation. The two electrodes of the sensor are the working and counter electrode and an external MSE reference electrode is used. Electrochemical characterisation is performed in an aqueous H_2SO_4 solution
b Two-electrodes configuration used for the testing of the sensor in gas phase. The gas flows in the chamber, no liquid is present except the water in the *Nafion* and SU-8 layers

sensor showed in Fig. 1*a* in a hard contact mode. The 100 nm thick Pt electrodes were deposited via e-beam evaporation at a rate of 1 Å s^{-1}, and the resist was stripped in acetone.

Prior to characterisation and testing, the *Nafion* layer needs to be rehydrated and acidified in order to have optimum proton conductivity. The sensor is thus immersed in a series of baths at 80°C for 15 min each: (i) H_2O_2 2%vol. in H_2O, (ii) H_2SO_4 0.1 mol l^{-1} and (iii) H_2O. After that treatment the sensors are ready to be characterised and tested. A cross-section of the sensor is presented in Fig. 1*b*.

2.3. Characterisation and test methods: The topological characterisation of the sensor was made with a profilometer and the results are presented in Table 1. The given thicknesses are the mean values measured across a full wafer. Concerning the *Nafion* layer, the measurement of its thickness revealed a quite important irregularity spanning from 300 to 600 nm across the wafer that had an important impact on the yield of sensors per wafers.

The sensors are first characterised as a conventional electrochemical cell in a three-electrodes configuration. The characterisation setup is presented in Fig. 2*a* and represents the sensor with its two electrodes being the working and counter electrodes, connected to an external *mercury/mercury sulphate electrode (MSE)* reference electrode (E°_{MSE} = − 0.654 V against standard hydrogen electrode (SHE)) to a *Biologic*® SP-300 potentiostat. All three electrodes are immersed in a 0.1 mol l^{-1} H_2SO_4 solution and cyclic voltammetry (CV) is performed between various potential limits and at different sweep rates. In cyclic voltammetry, the potential (in volts) is applied and swept between the working and the counter electrodes. The corresponding current (in milliamperes) flowing between the working and counter electrodes is recorded and plotted against the voltage measured between the working and the reference electrode.

Testing of the sensors for the detection of CO is performed in a custom made test chamber presented in Fig. 2*b*. The electrodes are connected to the same potentiostat in a two-electrodes configuration. The test chamber is under constant gas flow from either pure N_2 or pure CO with a flow rate of 20 cm^3 min^{-1}. While the test chamber is under gas flow, the voltage is swept between the two electrodes of the sensor from −0.5 to 0.5 V with a 200 mV s^{-1} sweep rate. We choose that sweep rate because it allows to observe more intense current signals.

3. Results and discussion

3.1. Electrochemical characterisation: The electrochemical characterisation of the sensor consists of two experiments

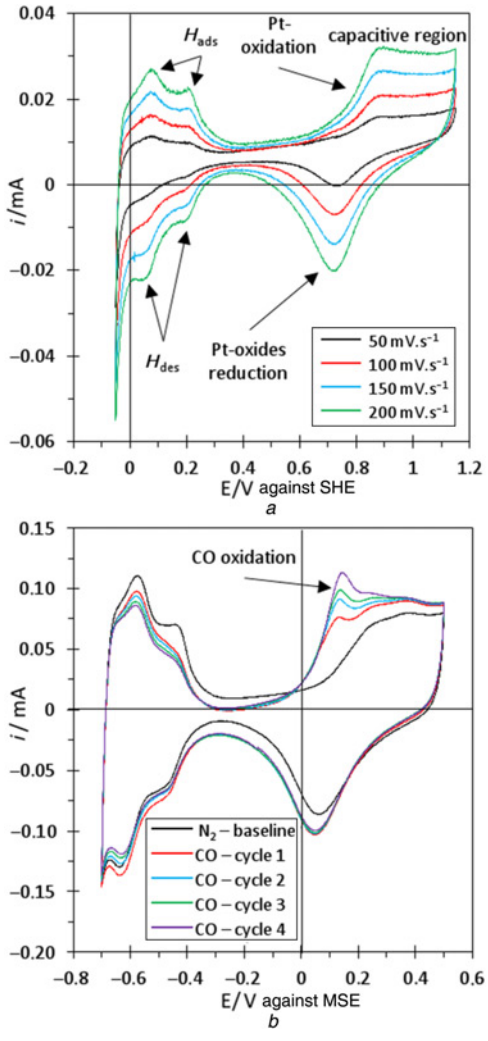

Fig. 3 *Electrochemical characterisation*
a Cyclic voltammetry at different sweep rates in the three-electrodes configuration, in H_2SO_4 0.1 mol l^{-1}. All typical signals from polycrystalline Pt in acidic medium are present and the signal increases with the sweep rate
b Cyclic voltammetry at 200 mV s^{-1} in H_2SO_4 0.1 mol l^{-1} with different gases bubbling in the cell. The signal of CO oxidation into CO_2 appears just before the capacitive region of Pt oxides

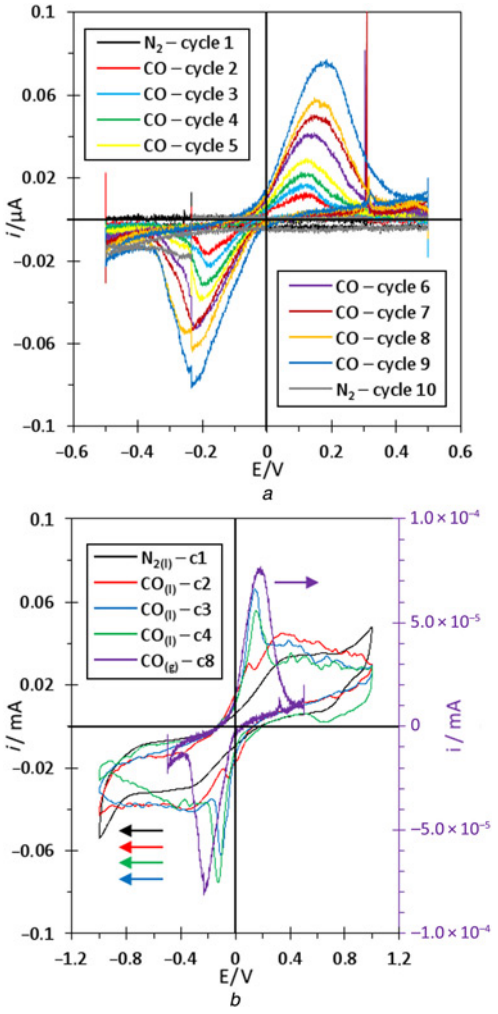

Fig. 4 *CO detection tests*
a Cyclic voltammetry of the testing of the sensor in the two-electrodes configuration in the gas phase under pure N_2 or CO flow
b Cyclic voltammetry obtained in liquid phase (H_2SO_4 0.1 mol l^{-1}), without external reference electrode, with N_2 bubbling (black) and pure CO bubbling (red, green and blue) and cycle 8 of *A* (purple) is superimposed for interpretation

doi: 10.1049/mnl.2016.0364

performed in the configuration of Fig. 2*a*. The first one is done with N_2 bubbling in the cell and the second one with CO bubbling.

The experiment with N_2 is necessary to check that the Pt electrodes surface is well exposed and available for redox reactions. The results are shown in Fig. 3*a* where one can see a typical CV curve for polycrystalline Pt in acidic medium [18]. The quality of the Pt surface as well as the ionic conductivity of the *Nafion* are confirmed by the presence of all expected electrochemical signals. The observed signals are H adsorption/desorption located between 0 and 0.25 V against SHE, the Pt oxide formation starting at 0.7 V against SHE, the capacitive region plateau and the Pt oxides reduction peak at 0.7 V against SHE. The experiment is conducted at several sweep rates from 50 to 200 mV s^{-1}. All electrochemical signals are increasing in current with the increasing sweep rate, which is expected in cyclic voltammetry experiments.

The second electrochemical characterisation is conducted in similar conditions, but with CO bubbling. The resulting curve is showed in Fig. 3*b*. One can see that the general shape of the curve is similar to the one obtained under N_2, but an oxidation peak appears at 0.15 V against MSE. This peak corresponds to the oxidation of CO into CO_2 according to its position on the potential scale when converted to the SHE scale [E(Pt) (CO_2/CO) $\simeq$ 0.8 V against SHE] [16]. The presence of this oxidation peak confirms that the sensor is indeed capable of detecting CO by measuring an increasing current at a specific applied potential corresponding to its redox potential. In addition to the presence of this oxidation peak, one can also see a slight decrease in the current at the H ads/des peaks. This phenomenon tends to confirm the nature of the oxidation of CO into CO_2 as the adsorption of CO on Pt occurs on the same catalytic sites as H [19].

3.2. CO detection tests: As model pollutant CO was chosen for the validation of the electrochemical capabilities of the sensor. The experiment is conducted on the setup showed in Fig. 2*b*. In Fig. 4*a*, as the voltage is cycled between −0.5 and 0.5 V with a 200 mV s^{-1} sweep rate, the gas flow is alternatively switched from N_2 to CO and to N_2 again. In this configuration, the voltage is swept from one limit to the other in 5 s, which means that the observed changes in signal are happening on that time scale. The first cycles under N_2 allows obtaining a baseline to better identify the signal obtained under CO. The last cycle under N_2 is to confirm that the response time is around 5 s.

The initial curve obtained under N_2 flow, Fig. 4*a* black line, shows low level of current and no signal as expected. When the CO flow is turned on, immediately an oxidation peak appears at 0.2 and −0.2 V with increasing current over cycles as the surface continues to be covered by CO. The charge of both peaks is almost identical, $\simeq$ 0.3 µC, which shows that they are probably the signal of the same redox process happening alternatively on both electrodes as the polarisation changes. As the gas flow is switched from CO to N_2 again, the oxidation signal disappears showing the good responsiveness of the sensor and that the surface becomes fully available once CO is no longer flown in the chamber.

Though there is only CO flowing in the test cell, in the absence of a reference electrode, absolute identification cannot be done. To confirm that the observed signal is indeed CO oxidation into CO_2, a similar experiment is performed in liquid environment.

The sensor is placed in the electrochemical cell with the same electrolyte as for characterisation (Fig. 2*a*), but this time without the reference electrode. Again, N_2 and then CO are bubbled into the cell, and the resulting curves are shown in Fig. 4*b*. In this two-electrodes configuration, all H related signals, observed in Fig. 3*a*, disappear and the curve becomes symmetrical with respect to 0 as are the curves obtained in the gas phase from Fig. 4*a*. The only signal which is observed under N_2 bubbling is the capacitive region. However, as CO is bubbled in the cell, an oxidation peak appears at 0.2 and −0.2 V, just before the capacitive region, as it was observed in Fig. 3*b*. This peak can be attributed to CO oxidation and its position in this configuration matches well with the position of the peak observed in the gas phase experiment (Fig. 4*a*).

Obtaining this curve confirms that the result from Fig. 4*a* is indeed CO getting oxidised in CO_2 and thus that the sensor is capable of performing electrochemical measurements in gaseous conditions. It also shows that it can be used to identify the molecule being adsorbed on the sensors unlike conventional metal–oxide-based sensors measuring a change in resistance, indicating that a specie is present, but cannot be identified [20].

4. Conclusion: In summary, the design and fabrication process of a microelectrochemical gas sensor were presented along with both topological and electrochemical characterisations. It has been showed that the sensor behaves as a typical working/counter electrodes couple when connected to an external reference electrode in a conventional electrochemical cell.

Testing of the sensor for the detection of CO as model pollutant has proved that the sensor is capable of electrochemical measurements in the gas phase.

To further improve the current sensor, the research effort is now focused on the implementation of a reference electrode in order to achieve identification of species directly in working conditions. Moreover, experiments in diluted gas as well as in mixtures of gases will allow to fully confirm the ability of the sensor to identify molecules.

5. Acknowledgments: Authors acknowledge the funding contribution of the *French Department of Defense (DGA)* and the *BioX*.

6 References

[1] Wan Q., Li Q.H., Chen Y.J., *ET AL.*: 'Fabrication and ethanol sensing characteristics of ZnO nanowire gas sensors', *Appl. Phys. Lett.*, 2004, **84**, (18), pp. 3654–3656

[2] Choi S.-W., Katoch A., Kim J.-H., *ET AL.*: 'Remarkable improvement of gas-sensing abilities in p-type oxide nanowires by local modification of the hole-accumulation layer', *ACS Appl. Mater. Interfaces*, 2015, **7**, (1), pp. 647–652

[3] Kida T., Seo M.-H., Suematsu K., *ET AL.*: 'A micro gas sensor using TiO_2 nanotubes to detect volatile organic compounds', *Appl. Phys. Express*, 2013, **6**, (4), p. 047201

[4] Hoefer U., Böttner H., Felske A., *ET AL.*: 'Thin-film SnO_2 sensor arrays controlled by variation of contact potential – a suitable tool for chemometric gas mixture analysis in the TLV range', *Sens. Actuators B, Chem.*, 1997, **44**, (1–3), pp. 429–433

[5] Liu X., Cheng S., Liu H., *ET AL.*: 'A survey on gas sensing technology', *Sensors*, 2012, **12**, (7), pp. 9635–9665

[6] Nguyen H., Quy C.T., Hoa N.D., *ET AL.*: 'Controllable growth of ZnO nanowires grown on discrete islands of Au catalyst for realization of planar-type micro gas sensors', *Sens. Actuators B, Chem.*, 2014, **193**, pp. 888–894

[7] Ng K.T., Boussaid F., Bermak A.: 'A CMOS single-chip gas recognition circuit for metal oxide gas sensor arrays', *IEEE Trans. Circuits Syst., Regul. Pap.*, 2011, **58**, (7), pp. 1569–1580

[8] Kumar D., Hashmi S.A.: 'Ionic liquid based sodium ion conducting gel polymer electrolytes', *Solid State Ion.*, 2010, **181**, (8–10), pp. 416–423

[9] Sun W., Shi Z., Liu M., *ET AL.*: 'An easily sintered, chemically stable, barium zirconate-based proton conductor for high-performance proton-conducting solid oxide fuel cells', *Adv. Funct. Mater.*, 2014, **24**, (36), pp. 5695–5702

[10] Mauritz K.A., Moore R.B.: 'State of understanding of *Nafion*', *Chem. Rev.*, 2004, **104**, (10), pp. 4535–4586

[11] Pálinkó I., Török B., Prakash G.K.S., *ET AL.*: 'Dehydration–rehydration characteristics of *Nafion*-H, *Nafion*-H supported on silica and *Nafion*-H silica nanocomposite catalysts studied by infrared microscopy', *J. Mol. Struct.*, 1999, **482–483**, pp. 29–32

[12] Nagao Y.: 'Highly oriented sulfonic acid groups in a *Nafion* thin film on Si substrate', *J. Phys. Chem. C*, 2013, **117**, (7), pp. 3294–3297

[13] Taylor A.D., Lucas B.D., Guo L.J., *ET AL.*: 'Nanoimprinted electrodes for micro-fuel cell applications', *J. Power Sources*, 2007, **171**, (1), pp. 218–223

[14] Shah K., Shin W.C., Besser R.S.: 'Novel microfabrication approaches for directly patterning PEM fuel cell membranes', *J. Power Sources*, 2003, **123**, (2), pp. 172–181
[15] Wang Y., Chen K.S., Mishler J., *ET AL.*: 'A review of polymer electrolyte membrane fuel cells: technology, applications, and needs on fundamental research', *Appl. Energy*, 2011, **88**, (4), pp. 981–1007
[16] Vidaković T., Christov M., Sundmacher K.: 'The use of CO stripping for in situ fuel cell catalyst characterization', *Electrochim. Acta*, 2007, **52**, (18), pp. 5606–5613
[17] Wouters K., Puers R.: 'Diffusing and swelling in SU-8: insight in material properties and processing', *J. Micromech. Microeng.*, 2010, **20**, (9), p. 95013
[18] Brett C.M.A., Brett A.M.O.: 'Electrochemistry principles, methods, and applications' (Oxford University Press, Oxford, New York, 1993)
[19] Marković N.M., Grgur B.N., Lucas C.A., *ET AL.*: 'Electrooxidation of CO and H_2/CO mixtures on Pt(111) in acid solutions', *J. Phys. Chem. B*, 1999, **103**, (3), pp. 487–495
[20] Sun Y.-F., Liu S.-B., Meng F.-L., *ET AL.*: 'Metal oxide nanostructures and their gas sensing properties: a review', *Sensors*, 2012, **12**, (3), pp. 2610–2631

doi: 10.1049/mnl.2016.0364